JOURNAL OF VIROLOGY, Dec. 1995, p. 7674–7681 Vol. 69, No. 12
0022-538X/95/$04.00+0

Mouse Adenovirus Type 1 Causes a Fatal Hemorrhagic Encephalomyelitis in Adult C57BL/6 but Not BALB/c Mice

JACK D. GUIDA,[1] GYORGY FEJER,[1]† LIISE-ANNE PIROFSKI,[1,2] CELIA F. BROSNAN,[3] AND MARSHALL S. HORWITZ[1,4,5]*

Departments of Microbiology and Immunology,[1] Pathology,[3] Medicine,[2] Pediatrics,[4] and Cell Biology,[5] Albert Einstein College of Medicine, Bronx, New York 10461

Received 10 July 1995/Accepted 7 September 1995

Mouse adenovirus type 1 (MAV-1) produces a lethal disease in newborn or suckling mice characterized by infectious virus and viral lesions in multiple organs. Previous reports of MAV-1 infection of adult mice generally described serologic evidence of infection without morbidity or mortality. However, our current results demonstrate that MAV-1 causes a fatal illness in adult C57BL/6 (B6) mice (50% lethal dose, [LD_{50}], $10^{3.0}$ PFU) but not in adult BALB/c mice at all of the doses tested (LD_{50}, $\geq 10^{5.0}$ PFU). Adult (BALB/c × B6)F_1 mice were intermediately susceptible (LD_{50}, $10^{4.5}$ PFU). Clinically, the sensitive B6 mice showed symptoms of acute central nervous system (CNS) disease, including tremors, seizures, ataxia, and paralysis. Light microscopic examination of CNS tissue from the B6 animals revealed petechial hemorrhages, edema, neovascularization, and mild inflammation in the brain and spinal cord. Analysis by electron microscopy showed evidence of inflammation, such as activated microglia, as well as swollen astrocytic endfeet and perivascular lipid deposition indicative of blood-brain barrier dysfunction. Outside of the CNS, the only significant pathological findings were foci of cytolysis in the splenic white pulp. Assessment of viral replication from multiple tissues was performed by using RNase protection assays with an antisense MAV-1 early region 1a probe. The greatest amounts of viral mRNA in MAV-1-infected B6 animals were located in the brain and spinal cord. Less viral message was detected in the spleen, lungs, and heart. No viral mRNA was detected in BALB/c mouse tissue, with the exception of low levels in the heart. Viral titers of organ tissues were also determined and were concordant with RNase protection findings on the brain and spinal cord but failed to demonstrate significant infectious virus in additional organs. Our experiments demonstrate that MAV-1 has a striking tropism for the CNS that is strain dependent, and this provides an informative in vivo model for the study of adenoviral pathogenesis.

Adenoviruses (Ads) are important human pathogens infecting a wide range of tissues, including the respiratory tract, the gastrointestinal tract, and the conjunctiva. Less common sites of Ad infection include the urinary tract, liver, and central nervous system (CNS) (20, 36, 39). The study of human Ad pathogenesis in vivo has been hindered by species specificity, although valuable information regarding the functions of genes in early region 3 has been obtained from the cotton rat model of human Ad pneumonia (14). Nonhuman Ad serotypes, however, are ubiquitous in many vertebrate species and provide an alternate approach for the study of Ad pathogenesis. Mouse Ad type 1 (MAV-1), first identified in 1960, is a well-characterized, nonhuman Ad that has been successfully used in vivo for pathogenesis studies (16, 21).

The organization of the MAV-1 genome is similar to that of the human Ads. Sequence information is now available for most of the early regions and portions of the late regions (2, 3, 30, 38, 41). Comparison of the sequences and transcription maps of MAV-1 and human Ad early regions 1 and 4 (E1 and E4, respectively) demonstrates some important differences in organization, but with an apparent general conservation of function (1, 22). Conversely, the E3 region, known to encode at least four proteins with immunomodulatory functions in the human Ads, is highly divergent in MAV-1 (30, 44). Transcription mapping of the MAV-1 E3 region has identified a series of three 5′ coterminal transcripts that do not encode obvious homologs of human Ad E3 gene products (4). The expression of one of the proteins from the MAV-1 E3 region has recently been demonstrated; however, it is unknown whether this protein has immunomodulatory effects (5).

Previous studies of the course of MAV-1 infection in immunocompetent mice have shown that the virus infects mice of any age but causes morbidity and mortality only in neonatal and suckling animals. Resistance to MAV-1 disease rapidly increases to adult levels between 14 and 27 days of age (42). Clinically, MAV-1-infected suckling mice have been reported to become lethargic initially and burrow into the cage bedding during the terminal stages of the disease (17). It is unclear whether the latter symptom was due to viral effects in the CNS or extreme lethargy resulting from the disseminated infection. Histopathologic analysis of tissue from suckling and neonatal animals has been reported to show focal necrosis in the kidneys, heart, spleen, and brain, with viral inclusions in the Purkinje cells of the cerebellum. Viral titers in these tissues parallel the extent of the pathologic findings, in that infectious virus can be isolated from affected organs (42). Other studies have examined MAV-1-induced pathology in the heart valves and adrenal glands of neonatal and suckling mice (6, 18, 24). A tropism for endothelial cells was noted in both of these studies.

Reports of MAV-1 disease in adult mice are inconsistent. Generally, disease has been in found only in immunocompro-

* Corresponding author. Mailing address: Albert Einstein College of Medicine, 1300 Morris Park Ave., Chanin Room 515, Bronx, NY 10461. Phone: (718) 430-2230. Fax: (718) 430-8702. Electronic mail address: horwitz@aecom.yu.edu.

† Present address: Department of Microbiology, Semmelweiss School of Medicine, Budapest, Hungary.

mised adult animals or with high-dose infections. Experimental MAV-1 infection of athymic C3H/HeN(*nu*/*nu*) nude mice caused a lethal wasting disease characterized by duodenal hemorrhage at viral doses from 10^2 to 10^5 PFU, whereas immunocompetent C3H/HeN(*nu*/+) mice were resistant to clinical disease at these doses. A dose of 10^6 or 10^7 PFU caused a fatal illness, whose nature was not described, by 5 days postinfection in both immunocompromised and immunocompetent mice (43). Similarly, MAV-1 infection of CB.17/SCID mice, which lack both B and T cells on primarily a BALB/c background, has been shown to cause a fatal disseminated infection characterized by Reye's syndrome-like hepatic lesions and duodenal hemorrhage without the CNS manifestations commonly associated with this illness in humans (7, 27a, 29).

There is no published evidence that MAV-1 causes encephalitis in immunocompetent adult mice. Because Ads are infrequently associated with meningoencephalitis in humans, only limited epidemiologic and clinical data are available regarding human Ad encephalitis syndromes (23, 36). One nonhuman Ad serotype has been shown to be a cause of encephalitis in foxes. Even before the isolation of Ads by Rowe et al. (32), Green et al. (15) described an epidemic of encephalitis among foxes in captivity caused by a filterable viral agent that was apparently different from the other known encephalitic fox virus, canine distemper virus. Further studies showed that the virus isolated and later called canine Ad type 1 is the most common cause of hepatitis in domesticated canines (21).

This report describes novel clinical and pathologic aspects of the disease caused by MAV-1 infection in several inbred strains of mice. We show that C57BL/6 (B6) and DBA/2J (D2) mice are susceptible to lethal MAV-1 hemorrhagic encephalomyelitis, with a 50% lethal dose (LD_{50}) of 10^3 PFU for B6 mice. BALB/c mice are resistant to any signs of MAV-1 neurologic disease or mortality at viral inocula up to the maximum obtainable dose (10^5 PFU). The virus appears to have a tropism for the CNS in the sensitive B6 strain. Significant viral mRNA and titers are found primarily in the brain and spinal cord with less or undetectable virus in non-CNS tissues. The observed strain differences provide a system that will be useful for understanding viral pathogenesis in general, within the CNS, as well as the host factors that affect Ad tissue tropism.

(The data in this report are from a thesis to be submitted in partial fulfillment of the requirements for the degree of Doctor of Philosophy in the Sue Golding Graduate Division of Medical Sciences, Albert Einstein College of Medicine, Yeshiva University.)

MATERIALS AND METHODS

Mice. Six-week-old male and female B6, D2, BALB/c, and (BALB/c × B6)F_1 mice were purchased from Jackson Laboratories and used for experimental infection within 1 week of arrival. Selected mice tested negative for serologic evidence of infection with MAV-1, MAV-2, murine coronavirus, Sendai virus, Theiler's murine encephalomyelitis virus, minute virus of mice, reovirus type 3, lymphocytic choriomeningitis virus, Hantaan virus, ectromelia virus, mouse pneumonitis virus, polyomavirus, mouse cytomegalovirus, mouse thymic virus, and lactate dehydrogenase-elevating virus prior to experimental infection, while serum from experimentally infected mice tested positive only for MAV-1.

Cells and virus. Murine L929 cells (L cells) were maintained in Dulbecco's modified Eagle's medium (DME; Gibco BRL) supplemented with 10% fetal calf serum, 2 mM glutamine, 50 U of penicillin per ml, and 50 μg of streptomycin per ml (DME/10). MAV-1-infected L cells were maintained in the same medium with the serum concentration reduced to 3% (DME/3).

MAV-1 was grown in L cells, and 10-fold serial dilutions of virus were plaqued on L cells to determine virus titers as previously described (29). Crude virus was aliquotted and stored at −70°C prior to use. Experiments, unless otherwise indicated, were performed with aliquots of a single crude preparation of MAV-1 with a titer of 5×10^5 PFU/ml. Additional experiments were performed with either a CsCl-purified laboratory virus strain (7×10^6 PFU/ml) or crude virus (1×10^6 PFU/ml) obtained from the second passage of the American Type Culture Collection (ATCC) MAV-1 reference strain.

Purified virus was prepared from MAV-1 grown in L-cell suspension cultures infected with 0.01 PFU per cell in Joklik's modified Eagle's medium supplemented with 10% bovine calf serum, glutamine, penicillin, and streptomycin as described above. At 5 days postinfection, cells were pelleted by centrifugation and virus was released from the cells by a single freeze-thaw cycle and extracted twice with Freon. Virus in the supernatant from the Freon extractions was purified twice by equilibrium centrifugation in continuous CsCl gradients as previously described (19). Purified virus was diluted in glycerol to 50% and stored at −20°C.

Experimental infections. For LD_{50} determinations, six-week-old B6, BALB/c, and (B6 × BALB/c)F_1 animals were infected by intraperitoneal (i.p.) injection (five animals per dose) of 10-fold serially diluted doses of MAV-1 in 200 μl of DME/3 and observed up to twice daily for morbidity and mortality. Certain doses were omitted for each of the groups on the basis of LD_{50} estimations in preliminary experiments. To determine the LD_{50}s of the ATCC reference and CsCl-purified laboratory MAV-1 strains, groups of three B6 mice were infected with 10-fold serial dilutions, from 10^2 to 10^6 PFU of each viral preparation in DME/3.

For monoclonal antibody (MAb) protection, five B6 mice per group received 200 μg of the following MAb or diluent alone i.p. 1 h prior to i.p. challenge with 5×10^3 PFU of MAV-1: 2D6, an anti-MAV-1 fiber neutralizing immunoglobulin G2a (Ig G2a) generated from an MAV-1-infected BALB/c mouse and quantitated as previously described (28), or a murine antiricin IgG2a MAb. Antibodies were diluted in phosphate-buffered saline (PBS) to 1 mg/ml prior to use.

To compare MAV-1 infection in B6, D2, and BALB/c mice for histopathology, RNase protection, and viral titrations, 6-week-old male B6 and BALB/c mice were injected i.p. with 5×10^3 PFU of MAV-1; control mice were mock infected. Animals of each strain were sacrificed at day 1 postinfection (p.i.) and at day 4 p.i., which was the last day before deaths would be expected to occur among the B6 mice. Preliminary experiments have shown that the onset of clinical disease can occur between days 3 and 5 at this dose in B6 animals. Additional animals were sacrificed when moribund and processed further (see below).

Histopathologic and ultrastructural studies. Portions of necropsied organs were immersion fixed in either Trump's fixative (spinal cord) or 10% neutral buffered formalin (all other tissues) for histopathologic analysis. Fixed tissue, with the exception of that from the spinal cord, was embedded in paraffin, and 5-μm sections were stained with hematoxylin and eosin for histopathologic examination.

Spinal cords were prepared for electron microscopic examination as previously described (11). Briefly, the tissue was immersed in Trump's fixative for at least 8 h, postfixed in 2% osmium tetroxide, dehydrated in alcohol, and embedded in Epon resin. Sections 1 μm thick were dry mounted onto glass slides and stained with toluidine blue. Areas of interest were selected during light microscopic examination, sectioned, collected on copper grids, and stained successively with uranyl acetate and lead citrate. Visualization and photography were performed with a JEOL 100S electron microscope.

RNase protection. Total RNA was isolated from freshly dissected, flash-frozen brain, spinal cord, spleen, lung, liver, kidney, intestine, skeletal muscle, and heart tissues by homogenization in a Polytron PT MR 3000 homogenizer (Brinkmann) in TRI reagent (Molecular Research Center) in accordance with the manufacturer's directions. The MAV-1 E1a probe was cloned by ligating the PCR product of the following two primers into the *Bam*HI-*Eco*RI sites of pSPORT1 (Gibco BRL): primer 183, 5′ CGGAATTCAACCTTACCAGTCAGACCGCG CAAG 3′; primer 184, 5′ CGGGATCCGTTTTGAGGACATGGATCTGCG GTG 3′. This probe contains MAV-1 sequences from nucleotides (nt) 603 to 760. The first exon of the MAV-1 E1a RNA is spliced at nt 752, thus generating a transcript that is capable of protecting a 149-nt fragment of the antisense probe; this protection differs in length from that which would result from unspliced RNA or residual genomic DNA contamination of the RNA samples. A template for the generation of antisense RNA was produced from this plasmid by digestion with *Bam*HI (Boehringer Mannheim), followed by phenol extraction and ethanol precipitation. The antisense E1a probe was transcribed in vitro with T7 RNA polymerase in the presence of 100 μCi of [γ-^{32}P]UTP (800 Ci/mmol, 20 mCi/ml; Amersham) by using the Ambion MAXIscript kit in accordance with the manufacturer's directions. The murine tri-β-actin probe (Ambion) was generated in a similar manner, except that its specific activity was reduced by a 50-fold reduction of labeled ribonucleotide. The probes were purified by electrophoresis on 4% polyacrylamide-urea gels prior to use in RNase protection assays, which were performed simultaneously with the MAV-1 E1a and β-actin probes by using the RNAP II kit (Ambion) in accordance with the manufacturer's directions. The protected E1a and β-actin fragments, along with controls, were separated on 4% polyacrylamide-urea gels, dried, and visualized by autoradiography on Kodak X-Omat film. The total probe, as observed in undigested controls adjusted for exposure times and loading, was always in excess of the specific signal, ensuring the quantitative nature of the assay.

Viral titrations. Portions of dissected brains, spleens, lungs, and, spinal cords were weighed, homogenized in PBS to a concentration of 50 mg of tissue per ml, subjected to three freeze-thaw cycles, and centrifuged at 600 × *g* to pellet insoluble debris. Serial dilutions of the tissue supernatants were assayed for plaques on L cells as described above (29). Results were corrected for tissue

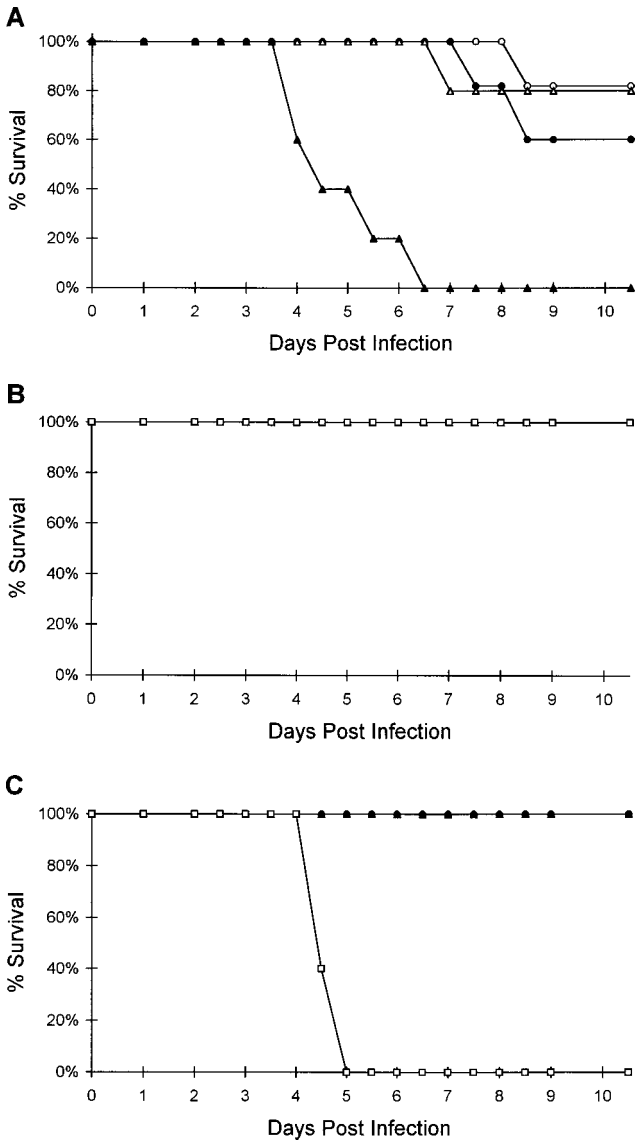

FIG. 1. Survival of MAV-1-infected B6 (A), BALB/c (B), and (BALB/c × B6)F_1 (C) animals. Groups of five mice were infected i.p. with 10-fold dilutions of MAV-1. Symbols: ○, 10^1 PFU; ●, 10^2 PFU; △, 10^3 PFU; ▲, 10^4 PFU; □, 10^5 PFU. There were no deaths beyond day 9 p.i.

weight and reported as the average number of PFU per gram of tissue plus the standard error of the mean for three mice per group.

RESULTS

Strain-specific differences in morbidity and mortality. Infection of B6 mice with 10^4 PFU of MAV-1 resulted in 100% mortality (five of five died). Symptoms occurred as early as 72 h p.i. and a lethal endpoint occurred within 48 h of the onset of symptoms (Fig. 1A). The first sign of disease in these mice was seizures, which developed between 3 and 5 days p.i. Within 12 to 24 h, these animals developed a hunched posture, ataxia, paresis, and, terminally, spastic and flaccid paralysis. The LD_{50} was 10^3 PFU for B6 mice, calculated from the mortality data by the method of Reed and Muench (31). Infection of B6 mice with doses from 10^1 to 10^3 PFU of MAV-1 resulted in 20 to 40% mortality (Fig. 1A) with a dose-dependent time of onset of clinical disease. The B6 animals that received lower virus doses experienced a delayed onset of symptoms, as late as 7 to 8 days p.i. These animals manifested additional neurologic symptoms, including tremors, bradykinesia, and athetosis. Most of the neurologic symptoms observed could be ascribed to damage of motor tracts or neurons in the spinal cord, brain stem, and cortex and to lesions in the cerebellum and basal ganglia.

BALB/c mice infected with doses of 10^3 to 10^5 PFU of MAV-1 did not develop clinical neurologic disease, nor did any succumb to lethal infection (LD_{50}, $\geq 10^5$ PFU) (Fig. 1B). At the highest dose (10^5 PFU), some clinical disease was evident. Three of five animals developed conjunctivitis, and all developed ruffled fur and hyperpnea. Continued observation of surviving B6 and BALB/c mice for up to 6 months p.i. revealed no evidence of late-appearing disease.

To begin to characterize the genetic factors involved in the host response to MAV-1 infection, (BALB/c × B6)F_1 mice were infected with 10-fold dilutions of MAV-1. F_1 animals infected with 10^5 PFU developed neurologic disease as early as 72 h p.i., and all succumbed within 24 to 48 h of the onset of symptoms. An LD_{50} of $10^{4.5}$ PFU was calculated from the data shown in Fig. 1C. At 10^4 PFU, several of the F_1 animals developed transient nonneurologic symptoms similar to those observed in BALB/c mice infected with 10^5 PFU. At doses of 10^2 and 10^3 PFU, no morbidity or mortality was observed.

Class I major histocompatibility complex haplotype does not determine susceptibility to MAV-1 infection. Since the *H-2* haplotypes of BALB/c and B6 mice differ, infection of D2 mice, which share the $H\text{-}2^d$ haplotype with the BALB/c strain, was used to assess the importance of the *H-2* haplotype in the observed strain differences in MAV-1 susceptibility. Ten D2 mice were infected with 5×10^3 PFU of MAV-1, a dose that is nearly 100% lethal for B6 mice but does not cause disease in BALB/c mice. At 4 to 6 days p.i., 10 (100%) of 10 D2 animals succumbed to a hemorrhagic encephalomyelitis that was indistinguishable, clinically and pathologically, from the disease observed in B6 animals (data not shown), demonstrating that *H-2*-encoded genes are not primary determinants of the MAV-1 susceptibility phenotype.

Specificity of MAV-1 in the etiology of CNS lesions. All of the B6 animals that received anti-MAV-1 fiber neutralizing MAb 2D6 were protected from MAV-1-induced morbidity or mortality when challenged with a lethal dose of virus (5×10^3 PFU). Both groups of five animals that received either the isotype control MAb or PBS succumbed to a fatal infection. This demonstrated that our laboratory strain of MAV-1 was required for the observed disease.

To examine the possibility that the laboratory strain of MAV-1 used in this study had either mutated towards increased neurovirulence or was contaminated with factors that could alter viral virulence, groups of 6-week-old B6 mice were infected with dilutions of a crude ATCC MAV-1 reference strain recently purchased and passed twice in our laboratory or CsCl-purified laboratory strain MAV-1. These animals were observed for morbidity and mortality; the results were similar to those of the infections with crude laboratory strain MAV-1 in terms of LD_{50} and clinical observations (data not shown). These results demonstrate that MAV-1 alone is sufficient to cause the observed syndrome and that the virus used in our studies is comparable to the ATCC MAV-1 reference strain.

Characterization of the differences between MAV-1 infections of B6 and BALB/c mice. In concordance with the LD_{50} experiment, the B6 mice infected with 5×10^3 PFU of MAV-1 for pathologic and virologic analysis began to show signs of illness as early as 3.5 days p.i. Neither the day 1 B6 animals nor any of the BALB/c mice showed signs of illness.

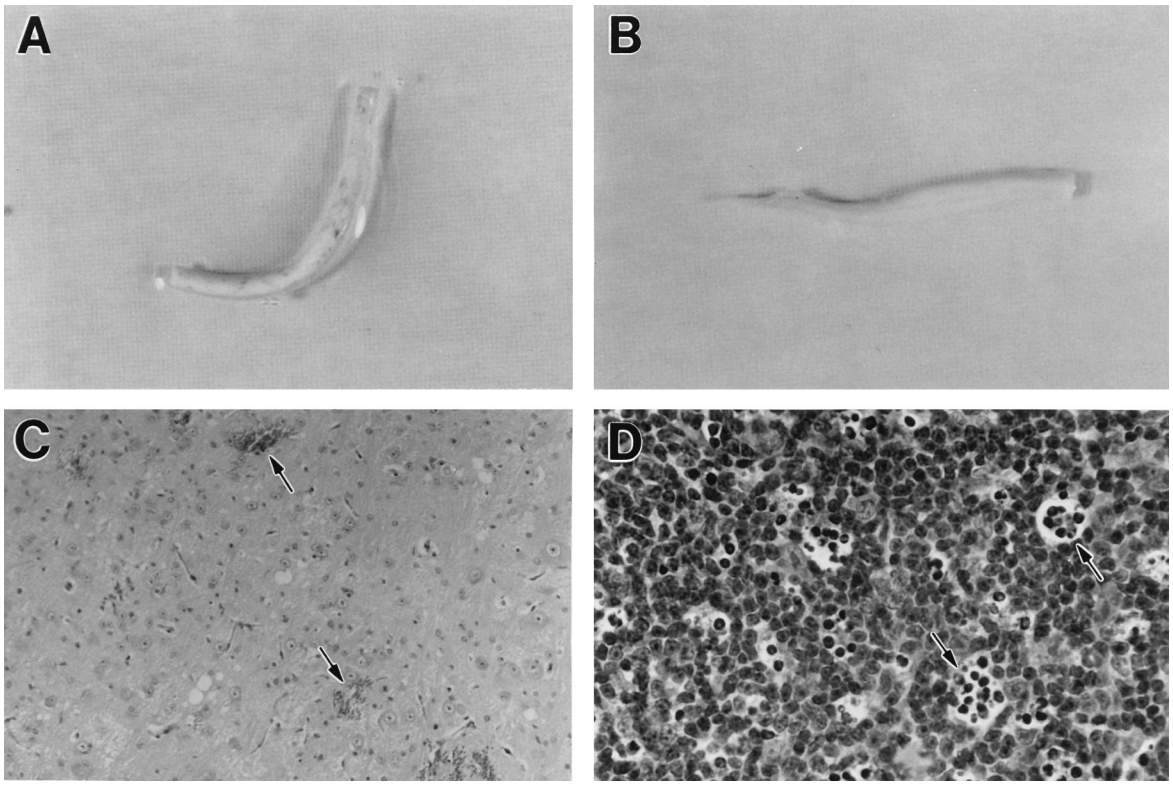

FIG. 2. Gross and histopathologic findings from mice infected with 5×10^3 PFU of MAV-1. A, B6 spinal cord, day 6 p.i.; B, BALB/c spinal cord, day 4 p.i.; C, B6 cerebral hemorrhages, several of which are designated by arrows, day 4 p.i. (magnification ×100); D, B6 spleen white pulp with foci of cytolysis, some of which are designated by arrows, day 4 p.i. (magnification, ×200).

(i) Pathologic analysis. Gross pathologic examination of internal organs revealed abnormalities in the CNS and spleens of B6 animals. The cerebella and spinal cords had numerous small surface hemorrhages (Fig. 2A). The number and size of these hemorrhages increased with the length of time p.i., on the basis of postmortem analysis of animals that died or were sacrificed with quadriplegia on days 5 and 6 p.i. The spleens of B6 animals were normal in size and had a dimpled surface. BALB/c animals had normal or slightly enlarged spleens with normal gross morphology. No evidence of hemorrhage was noted on the spinal cords of BALB/c mice (Fig. 2B).

Histopathologic examination of tissues from the B6 animals showed lesions in the CNS and spleens. Numerous focal hemorrhages were observed in the spinal cord and brain, primarily in the white matter (Fig. 2C). Edema was consistently observed throughout the CNS, as evidenced by clearings around vessels and pools of proteinaceous material in the white matter and gray matter of the spinal cord. Numerous endothelial cells appeared abnormal, containing large cytoplasmic vesicles and marginated chromatin. Neovascularization was frequently observed in the gray matter of the spinal cord, with an average of four to seven small vessels per high-power field. The nuclei of some neurons and astrocytes also had abnormal morphology, showing evidence of chromatolysis. Occasional areas of perivascular cuffing were observed, especially in the cerebellum. No hemorrhage, edema, or inflammation was seen in the CNS of infected BALB/c animals (data not shown).

The spleens of infected B6 animals had numerous foci of cytolysis in the white pulp (Fig. 2D) and a general decrease in the amount of red pulp. Whether these lesions represent direct viral cytopathology or an indirect effect of the viral infection is unclear from light microscopic analysis. BALB/c mouse spleens manifested evidence of proliferation, with large but normal-appearing germinal centers. No significant gross or light microscopic pathology was observed in the hearts, lungs, kidneys, intestines, or livers of any of the animals.

Electron microscopy of spinal cord sections of MAV-1-infected B6 animals from day 4 p.i. showed evidence of edema and inflammation. Swollen astrocytic endfeet and lipid droplets were observed surrounding vessels (Fig. 3A), while microglia with an activated appearance were found throughout the spinal cord (Fig. 3B). Tissue from BALB/c mice showed no detectable abnormalities by electron microscopy.

(ii) RNase protection. The highest levels of MAV-1 E1a expression were in the brains and spinal cords of B6 animals (Fig. 4). Lesser amounts were seen in spleen, lung, and heart tissues (Fig. 4 and data not shown). All of the other tissues examined (liver, kidney, and intestine) contained undetectable levels of MAV-1 E1a expression. No MAV-1 E1a message was detected by RNase protection in samples obtained from BALB/c mice on day 4 p.i., with the exception of a small amount in heart tissue, which was approximately equal to that in B6 mouse heart tissue.

(iii) Viral titrations. To determine infectious virus titers in brains, spinal cords, spleens, and lungs from MAV-1-infected B6 and BALB/c animals at day 4 p.i., organs were homogenized in PBS to 5% (wt/vol), clarified by centrifugation, and titrated on L cells. The results from three animals per datum point are shown in Fig. 5. In agreement with the RNase protection data, the highest titers were seen in B6 mouse brains and spinal cords. Little or no infectious virus was detected in B6 mouse spleens or lungs, however, which is discordant with

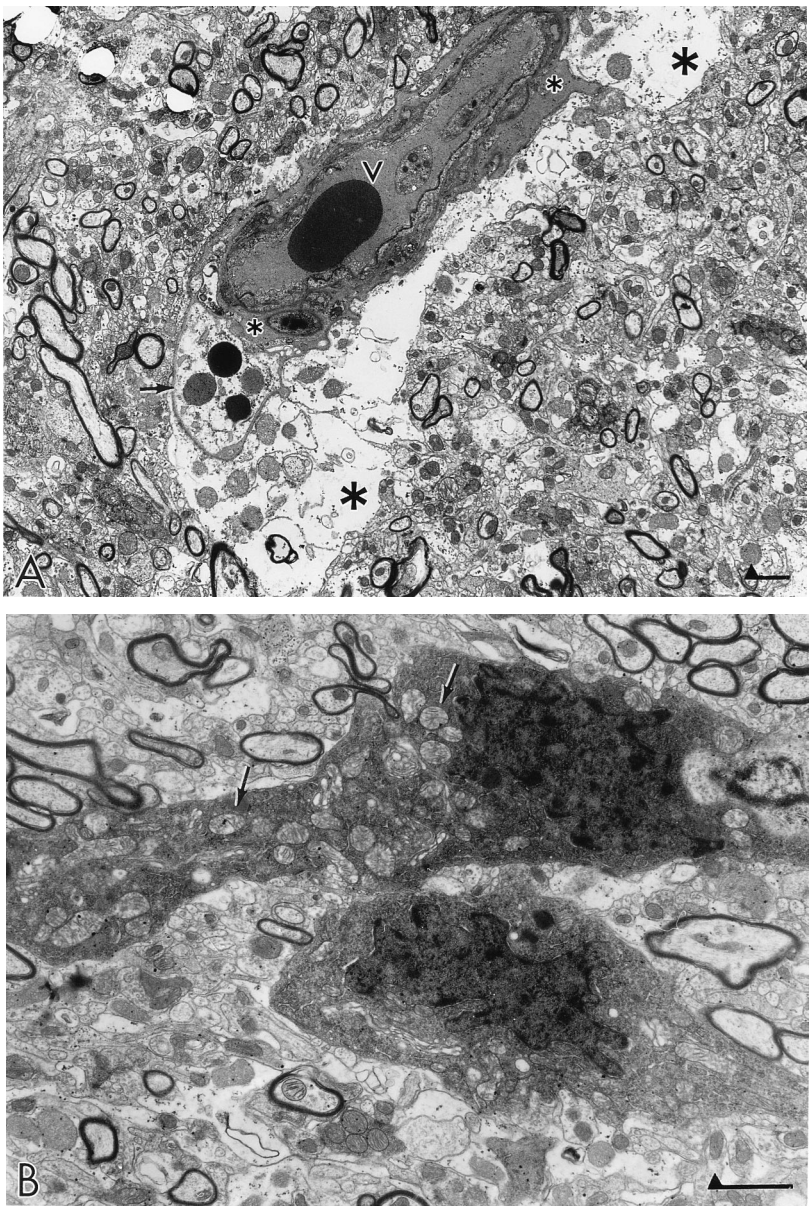

FIG. 3. Ultrastructural findings from spinal cords of B6 mice infected with 5×10^3 PFU of MAV-1 and examined on day 4 p.i. (A) Low-power field of a region of a dorsal column, showing myelinated nerve fibers, neurites, and a blood vessel (v). Damage to this vessel is evidenced by pools of proteinaceous material around the vessel (small asterisks) and edematous astroglial endfeet (large asterisks). (B) Two ramified microglia are seen among myelinated nerve fibers in the spinal cord. The cells appear reactive and have an unusually large number of mitochondria (arrows). Bars, 2 μm.

the significant histopathology observed in the spleen. No virus was detected in any of the BALB/c mouse tissues.

It is unlikely that the absence of virus titers in BALB/c mice was due to neutralizing antibodies in all of the homogenates, since serum neutralization titers were low or undetectable in all of the animals at the time of sacrifice (≤1:6 to 1:48; data not shown) and did not correlate with the susceptibility phenotype.

DISCUSSION

This is the first report of neurologic disease and hemorrhagic encephalomyelitis in MAV-1 infection of immunocompetent adult mice. We have demonstrated that the propensity of MAV-1 to cause CNS disease is strain specific, with neurologic disease occurring in B6 and D2 mice but not in BALB/c mice. (BALB/c × B6)F_1 mice have an intermediate MAV-1 susceptibility phenotype, demonstrating an incomplete dominance relationship between the genetic locus or loci responsible for the strain differences. Comparison of the D2 and BALB/c strains yielded additional genetic information. The fact that these strains share the same *H-2* haplotype (*H-2*^{d}) yet differ in susceptibility to MAV-1 CNS disease demonstrates that the *H-2* haplotype is not the primary basis for the differential strain susceptibility to MAV-1 CNS disease. Additionally, since MAV-1 CNS disease has not been previously reported in adult mice, we confirmed the MAV-1 etiology by showing that an MAV-1-specific neutralizing MAb was protective in vivo against a lethal challenge with the virus. We also showed that murine infection with CsCl-purified MAV-1 or the ATCC ref-

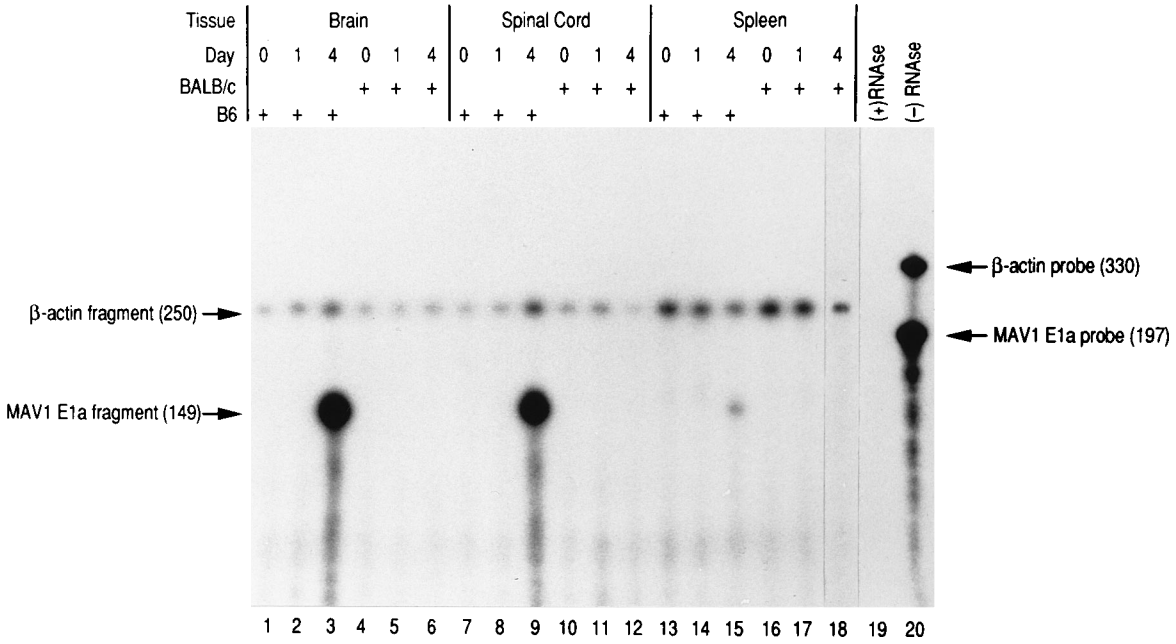

FIG. 4. Detection of MAV-1 transcription in various organs by RNase protection. B6 and BALB/c mice were infected with 5×10^3 PFU of MAV-1 and sacrificed on days 1 and 4 p.i. as described in Materials and Methods. Total RNAs were isolated from the brains, spinal cords, and spleens. Ten micrograms of total RNAs from the brains (lanes 1 to 6), spinal cords (lanes 7 to 12), and spleens (lanes 13 to 18) of uninfected (day 0) mice and mice infected for 1 and 4 days were analyzed by RNase protection simultaneously with an antisense MAV-1 E1a probe and a control antisense mouse β-actin probe. The MAV-1 E1a probe includes 158 nt of the MAV-1 sequence, of which 149 nt are included in the spliced E1a message, along with 39 nt of a nonviral plasmid sequence. The β-actin probe comprises 330 bases, 250 of which are protected by the mRNA for the nonmuscle isoform of the gene. The last two lanes each represent 1/80 of the total probe included in each reaction hybridized with yeast RNA and digested (lane 19) or not digested (lane 20) with RNase.

erence virus strain caused a disease indistinguishable from that caused by infection with laboratory-passaged MAV-1.

Comparison of the courses of MAV-1 disease in adult B6 and BALB/c mice showed that these strains respond differently, quantitatively and qualitatively, to MAV-1 infection. The difference in LD_{50} between the two strains is greater than 100-fold. Comparison of the clinical, pathologic, and virologic parameters of MAV-1 infection in these mice also suggests that the tissue tropism of MAV-1 in the two strains is different. It is noteworthy that conjunctivitis and ruffled fur were only rarely observed in B6 mice at any of the viral doses, including 10^5 PFU in separate experiments (data not shown), while they were frequently observed in BALB/c mice infected with this dose. If these symptoms were due to the effects of sublethal infection and not differences in tissue tropism, then it would have been predicted that the B6 mice would manifest these symptoms at the lower doses, and this was not observed. Previous studies of MAV-1 infection of another strain, B- and T-cell-deficient mice with severe combined immunodeficiency, which were derived from BALB/c mice and are congenic for a single B6 locus, failed to show any evidence of disease in the brain, even in the absence of antigen-specific immunity (29). This suggests that the observed strain differences are due not to differences in B- and T-cell immunity but rather to differences in viral receptor expression, tissue permissivity for MAV-1 infection, or differential efficacy of non-antigen-specific immunity, such as cytokine, macrophage, or natural killer cell activity.

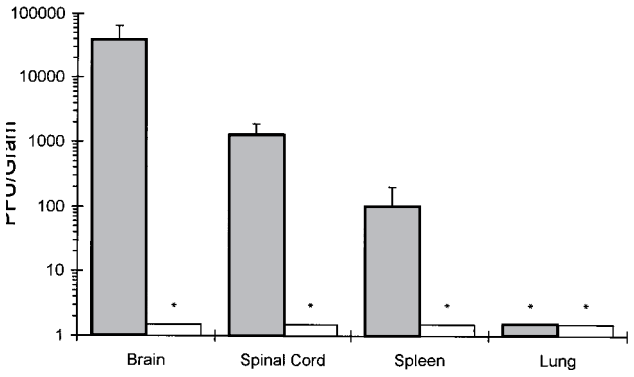

FIG. 5. MAV-1 titers in brain, spinal cord, spleen, and lung tissues from B6 and BALB/c mice at 4 days p.i. with 5×10^3 PFU of MAV-1, expressed in PFU per gram of tissue on a logarithmic scale. Titers were obtained by serial-dilution plaque assay on L cells with clarified tissue homogenates at a concentration of 50 mg of tissue per ml as described in Materials and Methods. Each point represents the average titer plus the standard error of the mean from three animals. The minimum detectable titer in this assay was 33 PFU/g of tissue. Asterisks indicate samples from which no viral plaques were obtained.

The results of previous studies showing sensitivity to disseminated MAV-1 disease in all of the murine strains tested when infected prior to 3 weeks of age strengthens the argument that immunologic differences can be the basis for strain differences (16, 17, 37, 42). This is based on the fact that the development of resistance to MAV-1 clinical disease correlates with the maturation of the murine immune system (8, 12, 40). An immunopathologic etiology remains another possibility that cannot be ruled out on the basis of currently available information. The use of immunodeficient mouse strains from other genetic backgrounds, such as the RAG1 and RAG2 knockouts (25, 35), or immunosuppression of B6 mice prior to MAV-1 infection could be informative in this regard.

Pathologic examination of tissue from MAV-1-infected B6 mice, in concordance with the clinical observations, showed a

picture of hemorrhagic encephalomyelitis. We observed that the number and size of the hemorrhages seen grossly on the spinal cords from moribund, quadriplegic animals increased with increasing time p.i. However, there were some animals with extensive spinal cord hemorrhages that were not quadriplegic, presumably because vital motor tracts of the spinal cord and brain were relatively spared at the time of postmortem examination. Electron microscopy showed abundant activated microglia and perivascular edema. The precise cause of the microglial activation is not clear, but it is possible that the viral infection stimulated the local production of cytokines, such as tumor necrosis factor alpha or gamma interferon, that have been shown to activate these cells. Microglia, once activated, are known to secrete a number of cytokines and other proinflammatory agents, including interleukins 1β and 6 and nitric oxide, which may be responsible for some of the changes in the CNS vasculature (9, 11, 13).

RNase protection analysis of MAV-1-infected B6 mice showed that the level of MAV-1 transcripts was highest in the brain and spinal cord, with less in the spleen, lungs, and heart. Little or no message was detected in the other organs examined. RNase protection has the advantage of proving that virus present in the tissue is metabolically active rather than simply physically trapped within the tissue; in addition, it can detect abortive viral replication cycles that fail to progress to production of progeny virus particles. The RNase protection data correlate with the brain and spinal cord viral titers, which were high. Surprisingly, however, only a very low virus titer was detected in the spleen, even though the pathologic changes were pronounced in this organ. The foci of degenerating cells in this organ had an appearance consistent with an apoptotic process but may also have represented viral cytopathology. One possible explanation for this discrepancy between the virologic and pathologic data is that the virus undergoes an abortive replication cycle in this tissue, terminating in the death of the host cell but without progeny virion production. An alternate hypothesis is that the virus directly or indirectly induces cytokine- or cell-mediated cytotoxicity against cells of the splenic white pulp.

The genetics underlying the observed MAV-1 susceptibility differences in the B6 and BALB/c strains are unclear. A number of possibilities are suggested by studies using other viral and nonviral pathogens in which strain-related differences in virulence were observed. For example, susceptibility to mouse cytomegalovirus-induced disease is determined by both *H-2*-linked and non-*H-2*-linked genes (10). The *cmv1* locus, which has been shown to be linked to the natural killer cell gene cluster on mouse chromosome 6, was identified as the factor controlling splenic mouse cytomegalovirus replication in B6 and BALB/c mice (33). Further experiments with mouse cytomegalovirus, guided by the genetic data, have shown more definitively that NK cells are the basis of the strain susceptibility difference (34). In contrast, susceptibility to hemorrhagic encephalitis caused by PVC-211, a mutant Friend murine leukemia virus molecular clone, differs between BALB/c and Swiss mice (26). This difference may be due to brain endothelial cell receptor differences, as revealed by sequence data that implicate a point mutation in the viral *env* gene as the viral neurovirulence factor (27). A better understanding of the genetics of MAV-1 susceptibility would be gained by experimental infection of F_2 and ($F_1 \times$ B6) backcross mice with 10^4 PFU of MAV-1. We have shown that this dose can discriminate between B6-like susceptible mice and F_1-like intermediately resistant animals (Fig. 1A and B).

In summary, we have found that MAV-1 causes hemorrhagic encephalomyelitis in adult mice of the B6 and D2 strains but not in those of the BALB/c strain, indicating a genetic basis for MAV-1 susceptibility that is unlinked to the *H-2* region. F_1 animals have an intermediate phenotype. Pathologic changes and viral mRNA are found primarily in the CNS of susceptible animals, with additional pathology in the spleen that does not appear to be due to infectious virus production. Further work should help identify the genetic and immunologic factors responsible for the strain differences observed.

ACKNOWLEDGMENTS

M.S.H. was supported by Cancer Center grant PO1 CA-13330. J.D.G. was supported by Medical Scientist Training grant 5T32 GM07288 from the National Institutes of Health. C.F.B. was supported by National Institutes of Health grant NS-11920.

We thank Clemens Cayetano for preparation of material for electron microscopy and Dinah Carrol for preparation of material for light microscopy.

ADDENDUM IN PROOF

Similar clinical and pathologic evidence of central nervous system infection with MAV-1 in outbred Swiss mice was observed recently by Kring et al. (S. C. Kring, C. S. King, and K. R. Spindler, J. Virol. **69:**8084–8088, 1995).

REFERENCES

1. **Ball, A. O., C. W. Beard, S. D. Redick, and K. R. Spindler.** 1989. Genome organization of mouse adenovirus type 1 early region 1: a novel transcription map. Virology **170:**523–536.
2. **Ball, A. O., C. W. Beard, P. Villegas, and K. R. Spindler.** 1991. Early region 4 sequence and biological comparison of two isolates of mouse adenovirus type 1. Virology **180:**257–265.
3. **Ball, A. O., M. E. Williams, and K. R. Spindler.** 1988. Identification of mouse adenovirus type 1 early region 1: DNA sequence and a conserved transactivating function. J. Virol. **62:**3947–3957.
4. **Beard, C. W., A. O. Ball, E. H. Wooley, and K. R. Spindler.** 1990. Transcription mapping of mouse adenovirus type 1 early region 3. Virology **175:**81–90.
5. **Beard, C. W., and K. R. Spindler.** 1995. Characterization of an 11K protein produced by early region 3 of mouse adenovirus type 1. Virology **208:**457–466.
6. **Blailock, Z. R., E. R. Rabin, and J. L. Melnick.** 1967. Adenovirus endocarditis in mice. Science **157:**69–70.
7. **Bosma, G. C., R. P. Custer, and M. J. Bosma.** 1983. A severe combined immunodeficiency mutation in the mouse. Nature (London) **301:**527–530.
8. **Burns, T. M., J. A. Clough, R. M. Klein, G. W. Wood, and N. E. Berman.** 1993. Developmental regulation of cytokine expression in the mouse brain. Growth Factors **9:**253–258.
9. **Campbell, I. L., C. R. Abraham, E. Masliah, P. Kemper, J. D. Inglis, M. B. Oldstone, and L. Mucke.** 1993. Neurologic disease induced in transgenic mice by cerebral overexpression of interleukin 6. Proc. Natl. Acad. Sci. USA **90:**10061–10065.
10. **Chalmer, J. E., J. S. Mackenzie, and N. F. Stanley.** 1977. Resistance to murine cytomegalovirus linked to the major histocompatibility complex of the mouse. J. Gen. Virol. **37:**107–114.
11. **Claudio, L., J. A. Martiney, and C. F. Brosnan.** 1994. Ultrastructural studies of the blood-retina barrier after exposure to interleukin-1 beta or tumor necrosis factor-alpha. Lab. Invest. **70:**850–861.
12. **Coutinho, G. C., S. Delassus, P. Kourilsky, A. Bandeira, and A. Coutinho.** 1994. Developmental shift in the patterns of interleukin production in early post-natal life. Eur. J. Immunol. **24:**1858–1862.
13. **Dickson, D. W., S. C. Lee, L. A. Mattiace, S. H. Yen, and C. Brosnan.** 1993. Microglia and cytokines in neurological disease, with special reference to AIDS and Alzheimer's disease. Glia **7:**75–83.
14. **Ginsberg, H. S., U. Lundholm-Beauchamp, R. L. Horswood, B. Pernis, W. S. M. Wold, R. M. Chanock, and G. A. Prince.** 1989. Role of early region 3 (E3) in pathogenesis of adenovirus disease. Proc. Natl. Acad. Sci. USA **86:**3823–3827.
15. **Green, R. G., N. R. Ziegler, B. B. Green, and E. T. Dewey.** 1930. Epizootic fox encephalitis. I. General description. Am. J. Hyg. **12:**109–129.
16. **Hartley, J. W., and W. P. Rowe.** 1960. A new mouse virus apparently related to the adenovirus group. Virology **11:**645–647.
17. **Heck, F. C., Jr., W. G. Sheldon, and C. A. Gleiser.** 1972. Pathogenesis of experimentally produced mouse adenovirus infection in mice. Am. J. Vet. Res. **842:**841–846.
18. **Hoenig, E. M., G. Margolis, and L. Kilham.** 1974. Experimental adenovirus infection of the mouse adrenal gland. II. Electron microscopic observations.

Am. J. Pathol. **75:**375–394.
19. **Horwitz, M. S.** 1971. Intermediates in the synthesis of type 2 adenovirus deoxyribonucleic acid. J. Virol. **8:**675–683.
20. **Horwitz, M. S.** 1990. Adenoviruses, p. 1723–1740. *In* B. N. Fields, D. M. Knipe, R. M. Chanock, J. L. Melnick, M. S. Hirsch, T. P. Monath, and B. Roizman (ed.), Virology. Raven Press, New York.
21. **Ishibashi, M., and H. Yasue.** 1984. Adenoviruses of animals, p. 497–562. *In* H. S. Ginsberg (ed.), The adenoviruses. Plenum Press, New York.
22. **Kring, S. C., A. O. Ball, and K. R. Spindler.** 1992. Transcription mapping of mouse adenovirus type 1 early region 4. Virology **190:**248–255.
23. **Ladisch, S., F. H. Lovejoy, J. C. Hierholzer, M. N. Oxman, D. Strieder, G. F. Vawter, N. Finer, and M. Moore.** 1979. Extrapulmonary manifestations of adenovirus type 7 pneumonia simulating Reye syndrome and the possible role of adenovirus toxin. J. Pediatr. **95:**348–355.
24. **Margolis, G., L. Kilham, and E. M. Hoenig.** 1974. Experimental adenovirus infection of the mouse adrenal gland. I. Light microscopic observations. Am. J. Pathol. **75:**363–374.
25. **Mombaerts, P., J. Iacomini, R. S. Johnson, K. Herrup, S. Tonegawa, and V. E. Papaioannou.** 1992. RAG-1-deficient mice have no mature B and T lymphocytes. Cell **68:**869–877.
26. **Park, B. H., E. Lavi, and G. N. Gaulton.** 1994. Intracerebral hemorrhages and infarction induced by a murine leukemia virus is influenced by host determinants within endothelial cells. Virology **203:**393–396.
27. **Park, B. H., B. Matuschke, E. Lavi, and G. N. Gaulton.** 1994. A point mutation in the *env* gene of a murine leukemia virus induces syncytium formation and neurologic disease. J. Virol. **68:**7516–7524.
27a. **Pirofski, L.** Unpublished data.
28. **Pirofski, L., D. Hassin, A. Kholy, M. S. Horwitz, and M. Scharff.** 1990. Isotype and variable region gene utilization in neutralizing murine anti-adenovirus hybridomas, abstr. 482, p. 166. Program and abstracts of the 30th Interscience Conference on Antimicrobial Agents and Chemotherapy. American Society for Microbiology, Washington, D.C.
29. **Pirofski, L., M. S. Horwitz, M. D. Scharff, and S. Factor.** 1991. Murine adenovirus infection of SCID mice induces hepatic lesions that resemble human Reye's syndrome. Proc. Natl. Acad. Sci. USA **88:**4358–4362.
30. **Raviprakash, K. S., A. Grunhaus, M. A. El Kholy, and M. S. Horwitz.** 1989. The mouse adenovirus type 1 contains an unusual E3 region. J. Virol. **63:**5455–5458.
31. **Reed, L. J., and H. Muench.** 1938. A simple method of estimating fifty percent endpoints. Am. J. Hyg. **27:**493–497.
32. **Rowe, W. P., R. J. Huebner, L. K. Gillmore, R. H. Parrott, and T. G. Ward.** 1953. Isolation of a cytopathogenic agent from human adenoids undergoing spontaneous degeneration in tissue culture. Proc. Soc. Exp. Biol. Med. **84:** 570–573.
33. **Scalzo, A. A., N. A. Fitzgerald, A. Simmons, A. B. La Vista, and G. R. Shellam.** 1990. Cmv-1, a genetic locus that controls murine cytomegalovirus replication in the spleen. J. Exp. Med. **171:**1469–1483.
34. **Scalzo, A. A., N. A. Fitzgerald, C. R. Wallace, A. E. Gibbons, Y. C. Smart, R. C. Burton, and G. R. Shellam.** 1992. The effect of the Cmv-1 resistance gene, which is linked to the natural killer cell gene complex, is mediated by natural killer cells. J. Immunol. **149:**581–589.
35. **Shinkai, Y., G. Rathbun, K. P. Lam, E. M. Oltz, V. Stewart, M. Mendelsohn, J. Charron, M. Datta, F. Young, A. M. Stall, et al.** 1992. RAG-2-deficient mice lack mature lymphocytes owing to inability to initiate V(D)J rearrangement. Cell **68:**855–867.
36. **Simila, S., R. Jouppila, A. Salmi, and R. Pohjonen.** 1970. Encephalomeningitis in children associated with an adenovirus type 7 epidemic. Acta Pediatr. Scand. **59:**310–316.
37. **Smith, A. L., and S. W. Barthold.** 1987. Factors influencing susceptibility of laboratory rodents to infection with mouse adenovirus strains K 87 and FL. Arch. Virol. **95:**143–148.
38. **Song, B., K. R. Spindler, and C. S. Young.** 1995. Sequence of the mouse adenovirus serotype-1 DNA encoding the precursor to capsid protein VI. Gene **152:**279–280.
39. **Straus, S. E.** 1984. Adenovirus infections in humans, p. 451–496. *In* H. S. Ginsberg (ed.), The adenoviruses. Plenum Press, New York.
40. **Vivier, E., J. M. Sorrell, M. Ackerly, M. J. Robertson, R. A. Rasmussen, H. Levine, and P. Anderson.** 1993. Developmental regulation of a mucinlike glycoprotein selectively expressed on natural killer cells. J. Exp. Med. **178:** 2023–2033.
41. **Weber, J. M., F. Cai, R. Murali, and R. M. Burnett.** 1994. Sequence and structural analysis of murine adenovirus type 1 hexon. J. Gen. Virol. **75:**141–147.
42. **Wigand, R.** 1980. Age and susceptibility of Swiss mice for mouse adenovirus, strain FL. Arch. Virol. **64:**349–357.
43. **Winters, A. L., and H. K. Brown.** 1980. Duodenal lesions associated with adenovirus infection in athymic "nude" mice. Proc. Soc. Exp. Biol. Med. **164:**280–286.
44. **Wold, W. S. M., T. W. Hermiston, and A. E. Tollefson.** 1994. Adenovirus proteins that subvert host defenses. Trends Microbiol. **2:**437–443.